

Approaching Quantum Criticality in ferromagnetic $\text{Ce}_2(\text{Pd}_{1-x}\text{Rh}_x)_2\text{In}$ alloys

J.G. Sereni^{1*}, M. Giovannini², M. Gmez Berisso¹, A. Saccone²

¹ *Div. Bajas Temperaturas, Centro Atómico Bariloche (CNEA) and Conicet, 8400 S.C. Bariloche, Argentina*

² *Dipartimento di Chimica e Chimica Industriale, Università di Genova, I-16146 Genova, Italy*

(Dated: March 2, 2022)

Low temperature magnetic and thermal (C_m) properties of the ferromagnetic (FM) alloys $\text{Ce}_{2.15}(\text{Pd}_{1-x}\text{Rh}_x)_{1.95}\text{In}_{0.9}$ were investigated in order to explore the possibility for tuning a quantum critical point (QCP) by doping Pd with Rh. As expected, the magnetic transition observed at $T = 4.1\text{K}$ in the parent alloy decreases with increasing Rh concentration. Nevertheless it splits into two transitions, the upper being antiferromagnetic (AF) whereas the lower FM. The AF phase boundary extrapolates to $T_N = 0$ for $x_{cr} \approx 0.65$ whereas the first order FM transition vanishes at $x \approx 0.3$. The QC character of the $T_N \rightarrow 0$ point arises from the divergent T dependence of the tail of C_m/T observed in the $x = 0.5$ and 0.55 alloys, and the tendency to saturation of the maximum of $C_m(T_N)/T$ as observed in exemplary Ce compounds for $T_N \rightarrow 0$. Beyond the critical concentration the unit cell volume deviates from the Vegard's law in coincidence with a strong increase of the Kondo temperature.

* E-mail-address of corresponding author: jsereni@cab.cnea.gov.ar

PACS numbers: 75.20.Hr, 71.27.+a, 75.30.Kz, 75.10.-b

I. INTRODUCTION

The $\text{Ce}_{2\pm u}\text{Pd}_{2\mp y}\text{In}_{1-z}$ family of alloys shows an extended range of solid solution [1] with a peculiar magnetic behavior since the Ce-rich branch ($u > 0 > y$) behaves ferromagnetic (FM) whereas the Pd-rich ($y > 0 > u$) is antiferromagnetic (AF). Such a difference of magnetic structure under a small variation of the alloy composition indicates that the energies of both phases are very similar. Another evidence for the competition between magnetic structures in this type of compounds is given by $\text{Yb}_2\text{Pd}_2\text{In}_{1-x}\text{Sn}_x$ [2], which orders magnetically at intermediate x values despite stoichiometric limits are not magnetic. Consequently this family of alloys are appropriated materials for testing the stability of exotic order parameters.

For this work, we have profited from the FM character of the $\text{Ce}_{2.15}\text{Pd}_{1.95}\text{In}_{0.9}$ composition to search for a quantum critical point (QCP) [3, 4] by tuning the chemical potential through the doping of the Pd lattice with Rh, like in the previously studied pseudobinary compound $\text{CePd}_{1-x}\text{Rh}_x$ [5]. For such a purpose, we have investigated the low temperature properties through magnetic (M) and specific heat (C_P) measurements performed on the Rh doped $\text{Ce}_{2.15}(\text{Pd}_{1-x}\text{Rh}_x)_{1.95}\text{In}_{0.9}$.

II. EXPERIMENTAL AND RESULTS

This alloyed system forms continuously all along the complete Pd/Rh concentration range with the $\text{Mo}_2\text{B}_2\text{Fe}$ type crystalline structure. The samples

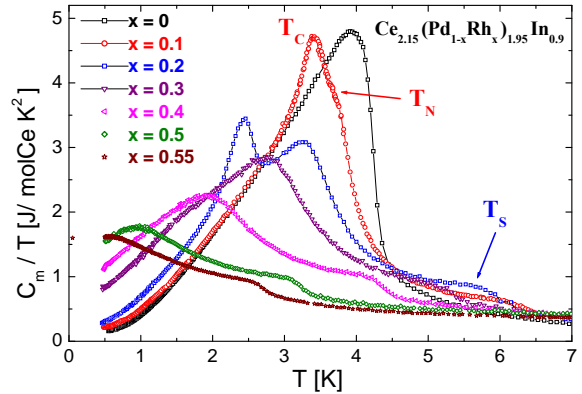


FIG. 1: Thermal and concentration dependence of the magnetic contribution to the specific heat divided temperature. T_C and T_N represent respective FM and AF transitions whereas T_S identifies a concentration dependent satellite transition discussed in the text.

were prepared using a standard arc melting procedure under an argon atmosphere, and remelted several times to ensure good homogeneity. The range of concentration investigated in this work covers more than 50% of the total Rh by Pd substitution, i.e. $0 \leq x \leq 0.55$. From structural properties, one observes that the volume of the unit cell decreases with Rh content following a Vegard's law up to $x = 0.3$. Beyond that concentration the volume decreases faster indicating that hybridization effect become relevant. The main change observed as a function of concentration occurs along the c-

axis.

The low temperature behavior was investigated on thermal and magnetic properties. Concerning $C_P(T)$ measurements, in Fig. 1 we present the thermal dependence of the magnetic contribution divided by temperature (C_m/T), after phonon subtraction for different concentrations extracted from the non-magnetic La isotypic reference compound.

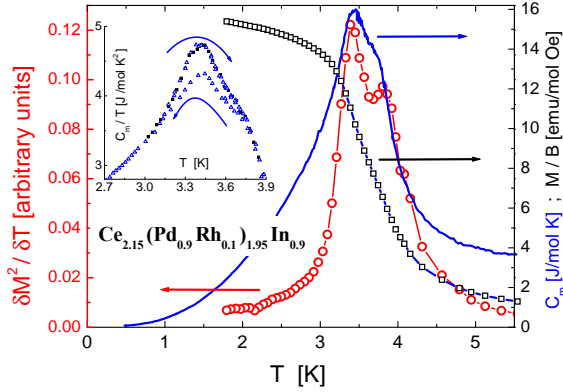


FIG. 2: Comparison between thermal derivative of $M^2(T)$ (left axis) with $C_m(T)$ (right axis) showing the split between FM and AF transitions. The original $M(T)$ dependence is also included (right axis). Inset: hysteresis of C_m/T between heating and cooling procedures.

As it can be seen in Fig. 1, the magnetic transition in the parent compound at $x = 0$ shows the characteristic C_m/T jump of second order character. However, a slight broadening at the maximum of C_m/T develops, which was previously interpreted as an intrinsic experimental broadening [1]. The new results indicate that the sample at $x = 0$ is actually close to a bi-critical point at $T_{cr} = 4.1$ K since the phase boundary splits into two transitions by Rh doping. Similar situation was found in the well known $\text{CeRu}_2(\text{Ge}_{1-x}\text{Si}_x)_2$ system [6]. Also in Fig. 1 a Rh concentration dependent satellite anomaly (T_S) is observed. The intrinsic character of this satellite transition is discussed below.

Magnetic $M(T)$ measurements on the $x = 0$ sample do not improve the identification of the bi-critical point because the FM signal largely exceeds the underlying AF cusp. The presence of this bi-critical point is not surprising if we consider a previous work [7] on the $\text{Ce}_{2\pm u}\text{Pd}_{2\mp y}\text{In}_{1-z}$ family of alloys. From that study, it concludes that $T_{cr} = 4.1$ K, lies in the extrapolated values of $T_N(y)$ from the Pd-rich AF samples (i.e. $Pd \geq 2 + y$) to the Ce-rich FM-branch (i.e. $Pd \geq 2 - y$). The same coincidence is observed for the paramagnetic tem-

perature θ_P extrapolated to $Pd = 1.95$ from the $Pd \geq 2$ side.

In the following we will analyze the evolution of the low temperature properties for further increase of the Rh content. The splitting between T_N and T_C becomes more clear in the thermal and magnetic results from the $\text{Ce}_{2.15}(\text{Pd}_{1-x}\text{Rh}_x)_{1.95}\text{In}_{0.9}$ sample at $x = 0.1$. That feature is observed as an incipient structure in the cusp of C_m/T , see Fig. 1 and Fig. 2. The first order character of the (lower) T_C transition is evidenced by an hysteresis at the $C_m(T)$ transition which shows a shift between heating or cooling procedures as depicted in the inset of Fig. 2.

A further evidence for the splitting of both phase boundaries is obtained from $M(T)$ measurements. Taking into account that from thermodynamic properties the internal magnetic energy U_m of a FM phase is related to the spontaneous magnetization, i.e. $U_m \propto M^2$, its temperature derivative $\partial M^2 / \partial T$ is proportional to $C_m(T)$ [8]. In Fig. 2 we compare both parameters (left axis for $\partial M^2 / \partial T$ and right axis for $C_m(T)$) showing that the mentioned structure at the transition is better defined by a $\partial M^2 / \partial T$ versus T dependence. The same features are observed in the $x = 0.2$ sample since the transitions increase their thermal difference ($T_N = 3.3$ K and $T_C = 2.5$ K) as observed in Fig. 1.

As it can be appreciated in Fig. 1, the nature of both transitions changes for $x \geq 0.3$. While $T_C(x)$ tends to vanish becoming a weak shoulder at $x = 0.3$, the $C_m(T_N)$ jump transforms into a broad maximum for $x \geq 0.4$ centered at 1.8 K ($x = 0.4$), 0.9 K ($x = 0.5$) and 0.5 K ($x = 0.55$) respectively. Those maxima are followed at higher temperature by a large tail resembling the non-Fermi-liquid behavior. Coincidentally, the value of the C_m/T maxima decrease and tends to saturate at around 1.5 J/molK² (see Fig. 1) as usually observed at the proximity of a QCP [9]. Particularly, sample $x = 0.55$ follows a power law divergency $C_m/T \propto 1/(T^{1.25} + 1)$ once the T_S anomaly is subtracted.

Concerning the satellite transition at $T_S(x)$, it can be mapped out to the T_C transition of the pseudo-binary compound $\text{CePd}_{1-x}\text{Rh}_x$ [5] at a similar Rh concentration. Coincidentally, the height of that anomaly nicely fits with the excess of Ce respect to the stoichiometric value, c.f. $2+u = 2+0.15$, that represents a 7.5% excess of Ce (remind that this compound contains 2 Ce atoms per formula unit). This observation is in agreement with the nearly constant entropy contribution of the anomaly. Both, $T_S(x)$ and entropy behaviors do not fit into a random concentration spurious contribution. This unexpected feature can

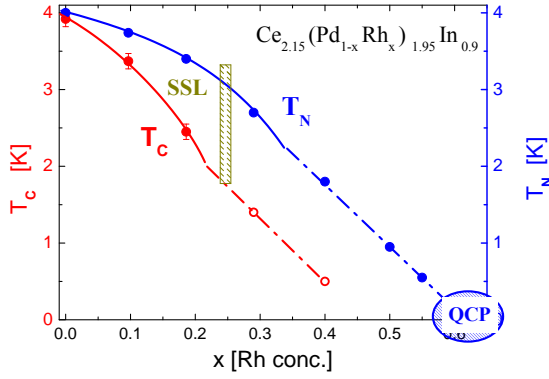


FIG. 3: Magnetic phase diagram showing $T_N(x)$ and $T_C(x)$ phase boundaries decrease. SSL indicates the region where a Shastry Sutherland lattice is expected to form.

be explained by analyzing the distribution of Ce atoms in this complex crystalline structure. As reported in Ref. [1] the Ce-plane, at $z = 0.5$, contains Ce atoms placed in the crystallographic site $4h$ whereas Ce atoms exceeding stoichiometric concentration (i.e. $u = 0.15$) replace In atoms at the $2a$ site at the $z = 0, 1$ planes. A further evidence for the intrinsic nature of this anomaly is given by scaling properties since for samples with $x \leq 0.4$ $C_m(x, T = T_S)$ nicely coincide if represented as a function of a normalized temperature $t = T/T_S$. $T_S(x)$ extrapolates to $T = 0$ for $x \approx 0.75$, beyond the studied concentration range. Preliminary magnetic measurements indicate that this anomaly is suppressed by the application of a moderate magnetic field ($B \approx 0.1$ T). Such a rapid suppression confirms that it is not due to a spurious $\text{CePd}_{1-x}\text{Rh}_x$ contribution because that compound has shown to behave differently under magnetic field [10].

III. MAGNETIC PHASE DIAGRAMS

In Fig. 3 we present the phase diagram showing that the upper (T_N) and the lower (T_C) transitions converge into a bi-critical point at $x \rightarrow 0$. Both boundaries are well defined for $x \leq 0.2$, but they broaden and smear respectively for $x \geq 0.3$. Since Rh doping effect is expected to introduce *holes* into the conduction band, in order to confirm the existence of that critical point we have

tested the possibility to move on the other direction, i.e. introducing more *electrons* into the band. For such a purpose we investigated the Ag doped alloy $\text{Ce}_{2.15}(\text{Pd}_{0.90}\text{Ag}_{0.10})_{1.95}\text{In}_{0.9}$, whose prelimi-

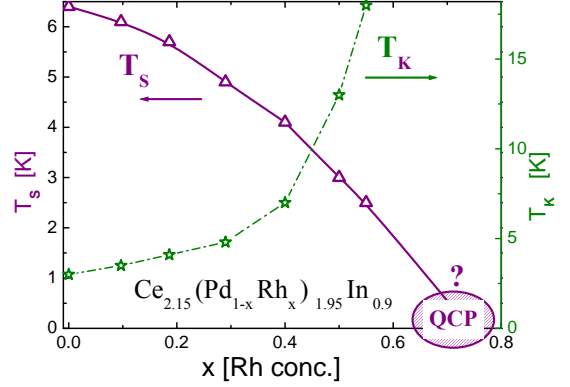


FIG. 4: Rh concentration dependence of the satellite anomaly T_S and the $T_K(x)$ increase (right axis).

nary thermal and magnetic properties indicate a clear FM behavior with the consequent disappearance on the AF phase at the bi-critical point.

From the magnetic behavior, the intermediate phase at $T_N \leq T \leq T_C$ seems to behave as a Shastry-Sutherland lattice [11], as it occurs in the isotypic compound $\text{Ce}_2\text{Pd}_2\text{Sn}$ [12]. This exotic phase, which requires of Ce-dimers formation, is suppressed once those dimers do not form anymore because of the weakening of Ce magnetic moments due to the arising Kondo screening.

Fig. 4 presents the concentration dependence of the satellite $T_S(x)$ anomaly with its extrapolation to $x \approx 0.75$, and the Kondo temperature $T_K(x)$ evaluated using the Desgranges-Schotte criterion [13]. According to this criterion, T_K can be computed as the temperature at which the entropy reaches the value $S(T_K) = 2/3R\ln 2$. It is worth noting that the rapid increase of $T_K(x)$ coincides with the extrapolation of $T_N(x)$ to the quantum critical point, and the deviation of $V(x)$ from the Vegard's law. On the contrary, the degrees of freedom involved in the $T_S(x)$ anomaly seems not to be affected by Rh increase at least up to $x = 0.55$, see Fig. 1. Further studies at higher Rh concentration are in progress to better determine $T_S(x)$ at lower temperature and its dependence on magnetic field.

- A., Ferro R., 2000, *Phys. Rev. B* **61** 4044.
- [2] Bauer E., Hilscher G., Michor H., Paul Ch., Aoki Y., Sato H., Adroja D.T, Park J.G., Bonville P., Godart C., Sereni J.G, Giovannini M., Saccone A., 2005 *J. Phys.: Condens. Matter* **17** S999.
- [3] Vojta T., 2000, *Ann. Phys. (Leipzig)* **9** 403.
- [4] Loehneysen H.v., Rosch A., Vojta M., Wölfle P., 2007, *Rev. Mod. Phys.* **79** 1015.
- [5] Sereni J.G., Westerkamp T., Gegenward P., Canales N., Geibel C., 2007, *Phys. Rev. B* **75** 024432.
- [6] Haen P., Biuod H., T. Fukuhara T., 1999, *Physica B* **259-261** (85).
- [7] Sereni J.G., Giovannini M., Gómez Berisso M., Saccone A., 2011, *Phys. Rev. B* **83** 064491.
- [8] See for example: Belov K.P., in *Magnetic Transitions*, Consultants Bureau Enterprises Inc., N.Y., 1961.
- [9] Sereni J.G., 2007, *J. Low Temp. Phys.* **147** 179.
- [10] Sereni J.G., Beaurepaire E., Kappler J.P., 1993, *Phys. Rev. B* **48** 3747.
- [11] See for example: Kim M.S., Aronson M.C., 2011, *J. Phys.: Condens. Matter* **23** 164204.
- [12] Sereni J.G., Gómez Berisso M. , Braghta A., Schmerber G., Chevalier B., Kappler J.P., 2009, *Phys. Rev. B* **80** 0244283 and 2010, *Phys. Rev. B* **81** 184429.
- [13] Desgranges H.-U. and Schotte K.D., 1982, *Physics Letters* **91A** 240.